ORIGINAL ARTICLE

Investigating Patient-Specific Absorbed Dose Assessment for Copper-64 PET/CT

Ali Abdulhasan Kadhim [1], Peyman Sheikhzadeh [1, 2*], Mehrshad Abbasi [2], Saeed Afshar [2], Nasim Vahidfar [2], Shirin Asidkar [3], Mehrnoosh Karimipourfard [4], Zahra Valibeiglou [5], Mohammad Reza Ay [1,6*]

[1] Department of Medical Physics and Biomedical Engineering, School of Medicine, Tehran University of Medical Sciences, Tehran, Iran

[2] Department of Nuclear Medicine, Imam Khomeini Hospital Complex, Tehran University of Medical Sciences, Tehran, Iran

[3] Nursing Care Research Center, Iran University of Medical Sciences, Tehran, Iran

[4] Department of Ray-Medical Engineering, Shiraz University, Shiraz, Iran

[5] Department of Medical Physics, School of Medicine, Tabriz University of Medical Sciences, Tabriz, Iran

[6] Research Center for Molecular and Cellular Imaging, Tehran University of Medical Sciences, Tehran, Iran

*Corresponding Authors: Peyman Sheikhzadeh, Mohammad Reza Ay
Email: psh82@yahoo.com, mohammadreza_ay@sina.tums.ac.ir

Received: 01 July 2024 / Accepted: 03 August 2024

Abstract

Purpose: There is a growing interest in the clinical application of new PET radiopharmaceuticals. This study focuses on using ^{64}Cu-DOTA-Trastuzumab for Positron Emission Tomography–Computed Tomography (PET/CT) imaging in gastric cancer patients. It aims to enhance the understanding of its bio-kinetic distribution and absorbed dose for safe and practical application in nuclear medicine.

Materials and Methods: The study was conducted at the Agricultural, Medical, and Industrial Research School (AMIRS), where ^{64}Cu was produced and purified. The radiopharmaceutical ^{64}Cu-DOTA-Trastuzumab was prepared, and three patients with confirmed Human Epidermal growth factor Receptor 2 (HER2)-positive gastric cancer underwent PET/CT scans at 1, 12 and 48 hours post-injection. Images were gained using a Discovery IQ PET/CT system and analyzed for an SUV. Bio-distribution was modeled using a two-exponential function, and absorbed doses were calculated using IDAC-Dose 2.1 software. CT doses were also evaluated.

Results: The study found that post-injection imaging at 12 hours or more provided superior image quality. The liver exhibited the highest cumulative activity, followed by the spleen and other organs. The effective dose estimates for ^{64}Cu-DOTA-Trastuzumab were within acceptable limits. CT dose calculations revealed that sensitive organs received higher doses.

Conclusion: This study successfully assessed the bio-kinetic distribution and absorbed dose of ^{64}Cu-DOTA-Trastuzumab in gastric cancer patients, demonstrating its safety and potential for clinical use. The optimal timing for PET/CT imaging and dosimetry data can inform clinical decision-making. Further research is warranted to explore the therapeutic potential of ^{64}Cu-DOTA-Trastuzumab and to establish clinical guidelines for its use.

Keywords: ^{64}Cu-DOTA-Trastuzumab; Internal Dosimetry; Positron Emission Tomography Computed Tomography; Absorbed Dose.

DOI: https://doi.org/10.18502/fbt.v13i1.20755

1. Introduction

Today, Positron Emission Tomography (PET) plays a crucial role in the medical field for diagnosing and tracking diseases. It typically offers a visual representation of how radioactive drugs spread across the body after being administered. Combining PET with Computed Tomography (CT) in a hybrid imaging technique known as PET/CT allows for merging detailed anatomical pictures with insights into bodily functions [1]. Many radioactive tracers have been created for potential application in medical imaging, yet ^{18}F-2-fluoro-2-Deoxy-D-Glucose (FDG) remains the sole PET tracer employed in standard clinical practice, especially for cancer imaging [2]. There is a growing interest in the clinical application of new PET radiopharmaceuticals employing metallic radionuclides, including ^{68}Ga, ^{89}Zr, and ^{64}Cu [3], particularly those with a longer half-life [4]. Over the past years, considerable research has studied the feasibility of using various copper radionuclides as versatile candidates in PET imaging and radionuclide therapy [5, 6].

Copper (Cu) is the third most abundant metal in the human body, essential for many biological processes. Changes in Cu levels often show various health conditions, including cancer and Alzheimer's disease, where they can serve as biomarkers. Neurodegenerative diseases are linked to either elevated or decreased levels of Cu. In cancer research, some observe that cancerous tissues exhibit increased copper concentrations and overexpression of the human copper transporter 1 (hCTR1) in various types of cancer cells, such as those found in melanoma, liver, lung, prostate, and glioblastoma [7]. So, it plays a vital role in detecting tumors, metastasis, and bone marrow lesions [8]. The initial production of a copper radiotracer took place at Washington University in St. Louis, USA, and was sent to the University of Alberta in Edmonton, Canada. Five of the 27 recognized copper radioisotopes are especially suitable for molecular imaging (^{60}Cu, ^{61}Cu, ^{62}Cu, and ^{64}Cu) and radiotherapy (^{64}Cu and ^{67}Cu). ^{64}Cu stands out as an ideal choice because of its 12.7-hour half-life and distinctive decay pattern, which includes beta plus (18%), beta minus (38%), and electron capture (44%). The emitted positron has an average energy of 278.2 keV and a maximum power of 653.0 keV, comparable to 18F with an average beta energy of 250 keV. The decay scheme of ^{64}Cu is illustrated in Figure [9]. Overall, ^{64}Cu is helpful for imaging and therapeutic applications [10]. Cu-64 has a longer half-life than F-18, which allows for more flexibility in radiopharmaceutical synthesis, transportation, and investigating biological processes over extended periods. This characteristic of Cu-64 makes it suitable for imaging agents that require time for biological targeting and for multi-center clinical trials; due to its coordination chemistry, Cu-64 can be used for a broader range of bioconjugation strategies, enabling the labeling of various biomolecules such as peptides, antibodies, and nanoparticles [11].

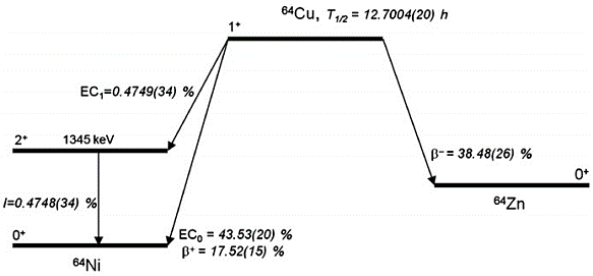

Figure 1. Decay mode schematic of ^{64}Cu

^{64}Cu can be used in various radiopharmaceutical forms (such as 64Cu-PSMA, ^{64}Cu-DOX, and ^{64}Cu-ATSM) for PET imaging and therapeutic purposes. Significant research is being conducted into its therapeutic applications. The substantial diagnostic capabilities of ^{64}Cu-PSMA imaging have been explored in prostate cancer patients experiencing recurrence and in the initial staging of select patients with advanced localized disease [12].

To achieve a targeted high dose of Doxorubicin (DOX) delivery to the lungs through intravenous injection, DOX was encapsulated within a chitosan-BSA multilayered hollow microcapsule constructed using a $CaCO_3$ template. The ^{64}Cu-DOX radiotracer was incorporated alongside non-radioactive DOX to assess the bio-distribution [13]. Tumor hypoxia is recognized for its role in enhancing malignant traits, such as resistance to therapy and the likelihood of metastasis. ^{64}Cu-diacetyl-bis (N 4-methyl thiosemicarbazone), also known as ^{64}Cu-ASTM, which can be labeled with various copper radioisotopes (^{60}Cu, ^{62}Cu, and ^{64}Cu), is a promising PET imaging agent designed to target hypoxic environments within tumors that exhibit reduced conditions [14]. In this respect, $^{64}CuCl_2$ is used for brain tumors [15] and prostate cancer imaging [16], ^{64}Cu-antibodies trastuzumab [17], and for breast cancer imaging and therapy. Despite the advantages

of ^{64}Cu's application in therapy, ^{64}Cu is not used as a standard treatment method and is mainly used for imaging. One reason for this problem may be insufficient information about the bio-kinetic distribution ^{64}Cu in tissues and its absorbed dose. This study aims to evaluate the bio-distribution and estimate the absorbed dose of ^{64}Cu-DOTA-Trastuzumab in gastric cancer patients through PET/CT imaging to improve safety and efficacy in nuclear medicine applications.

2. Materials and Methods

2.1. Preparation of ^{64}Cu-DOTA-Trastuzumab

The synthesis of 64Cu was achieved by the Ion Beam Separation Group at the Agricultural, Medical, and Industrial Research School (AMIRS). For this production, a zinc-68 (^{68}Zn) target was electroplated onto a high-purity gold-coated copper backing plate and then bombarded with a proton beam of 30 MeV. To refine the 64Cu produced, a cation exchange column was used, through which hydrochloric acid (25 mL/ 9 N) was passed at a rate of 1 mL/min. Subsequently, the resulting solution was processed through an anion exchange column using hydrochloric acid (50 mL/ 9 N) to achieve the purified ^{64}Cu [18].

Using an HPGe detector, Gamma spectroscopy was used to determine radionuclides' purity and assess the radiochemical purity. Two solvent systems were advantageous for this purpose: 1 mM diethylene-triamine-penta acetic acid (DTPA; $C_{14}H_{23}N_3O_{10}$) and a 10% ammonium acetate: methanol (1:1) mixture, which served as the mobile phases on Whatman paper No. 2 and silica gel, respectively, acting as the stationary phases. [^{64}Cu] Cu-DOTA-trastuzumab was synthesized by adding [^{64}Cu] $CuCl_2$ to an acetate buffer solution (pH: 7) containing DOTA-trastuzumab, followed by incubation for 1 hour at 40°C. The radiochemical purity of the [^{64}Cu] Cu-DOTA-trastuzumab radiolabeled compound was verified using HPLC and RTLC methods, yielding a radiochemical purity of 95±2% via ITLC and 99±0.5% via HPLC, with a specific activity ranging from 0.9–1.1 GBq/mmol.

2.2. Patients

Inclusion Criteria:

- Patients with proven pathology of stomach or breast cancer, with HER2 status confirmed by FISH or immunohistochemistry analysis.
- Individuals are at least 14 days away from recent chemotherapy or radiotherapy.
- Adequate kidney function is defined as creatinine clearance ≥ 50 ml/min (according to the Cockroft-Gault formula).
- Age ≥ 18 years.

Exclusion Criteria:

- Patients who declined PET/CT with 64Cu-DOTA-trastuzumab radiopharmaceutical after receiving necessary explanations and answering their questions.
- Individuals who discontinued participation in the program before the scan.
- Patients with uncontrolled diseases (such as fatal arrhythmias) require hospitalization.
- Pregnant or lactating women.
- Individuals with mental illnesses that impair decision-making and cooperation.
- Patients with physical conditions that disrupt the imaging process from a technical perspective.
- History of cancers other than stomach cancer.
- History of active inflammatory or infectious diseases.
- History of sensitivity or intolerance to trastuzumab.

Three patients with proven stomach cancer, referred to our nuclear medicine center between 2022 and 2023 for disease staging or follow-up, were included in the study. Before the scan, we reviewed the results of pathology and conventional imaging (MRI and CT), which were performed according to standard guidelines for gastric cancer screening. PET/CT scans using the ^{64}Cu-DOTA-trastuzumab radiopharmaceutical were performed at three intervals: 1, 12, and 48 hours after injection. The selected patients were over 18 years old, and their HER2 receptor expression status had been determined previously by IHC or FISH. Informed consent was obtained from all patients before the intervention.

2.3. PET-CT Imaging

The patients were scanned using a Discovery IQ PET/CT system (General Electric Healthcare, WI, USA). This system combines a high-sensitivity PET scanner, Bismuth Germanium Oxide (BGO) detectors, and a 16-slice CT scanner. Emission data were gained in list mode using an energy window of 350-650 keV and a coincidence timing window of 9.5 ns. Ordered Subset Expectation Maximization (OSEM) with Gaussian post-processing (OSEM+PSF) was used as a reconstruction algorithm. PET used a 70-cm FOV and a 192 × 192 matrix size, resulting in a 3.64 × 3.64 × 3.26 mm pixel size, while CT used 512×512 matrix size and KVp of 120 with smart mA to reduce patient dose.

2.4. Image analysis and Assessment of Feasibility

PET/CT images were stored in DICOM format and segmented using the Monaco Treatment Planning System (TPS) and Lifex software [19]. Expert radiologists segmented source organs, including the brain, heart, liver, lungs, kidneys, and spleen. The Segmented regions are depicted in Figure 2.

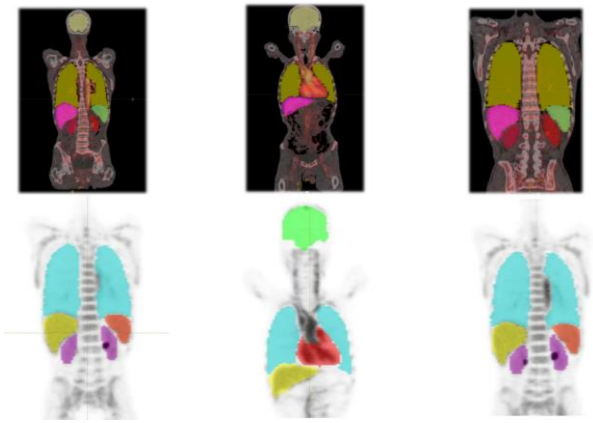

Figure 2. The segmented Organs in PET and CT images

2.5. Time Activity Curve Calculation

The acquired PET images were static, meaning no known kinetic information about the bio-distribution was available [20, 21]. We need to include bio-distribution models to get Time-Activity Curves (TAC) in each voxel, which will then obtain Cumulated Activities (CA) [22]. This research used a two-exponential function to determine the bio-distribution of the 64Cu in the body [23]. The Standard Uptake Value (SUV) [24] was calculated for each organ of each PET image series according to Equation 1, and the results were depicted as Curve (6).

$$\text{Activity Concentration in organ (Bq/ml)} = \frac{\text{Pixel Value}}{\text{Image Scale Factor}} \quad (1)$$

$$\text{SUV} = \frac{\text{Activity of each organ } (\frac{\text{mCi}}{\text{ml}})}{\frac{\text{Injected dose (mCi)}}{\text{Body Weight (g)}}} \quad (2)$$

Then, a two-exponential function was fitted on the obtained curve. The TAC for each organ was obtained through this curve fitting. The accumulated activity of each organ was obtained via the integral of TAC between 0, 12, and 48 h after injection. The accumulated activity of each voxel was calculated according to Equation 3 [21]:

$$C_{Ai} = CA_{organ} \frac{A_i^{pet}}{\sum_i^N A_i^{pet}} \quad (3)$$

Where CA_i is the accumulated activity in each voxel, CA organ is the accumulated activity of an exciting organ, A_i is the activity in each voxel, and ΣA_i^{PET} is the total activity in the same organ.

2.6. Radionuclide Absorbed Dose Calculations

This study used the IDAC-Dose 2.1 software to assess the absorbed organ dose and effective dose in our CU-64 trastuzumab patients [25]. The program encompasses 83 source regions and 47 target organs. For this investigation, we focused on the Kidneys, Lungs, Liver, and Spleen.

The biokinetic data for the ^{64}Cu-DOTA-Trastuzumab radiopharmaceutical were expressed as cumulative activity per administered activity (A/Ao), with the unit of measurement being hours (h). The cumulative activity within each organ was mathematically defined as follows (Equation 4):

$$\frac{\tilde{A}}{A_0} = F_s \sum_{i=1}^{n} a_i \frac{T_i,\ eff}{ln(2)}, Teff = \frac{T_i Tp}{T_i + Tp} \quad (4)$$

In this study, we considered the biological half-life of the nuclide (denoted as ai) and the fraction of the nuclide, Fs, and $T_{i,\ eff}$ as the uptake half-time. These parameters were incorporated into the IDAC-Dose 2.1

software based on the specific radiopharmaceutical type; then, we used the administered activity data for selected patients to calculate the effective dose based on the ICRP phantom [26].

2.7. CT Dose Assessment

Before the PET scan, a low-dose CT scan was conducted to generate CT Attenuation Correction (CTAC) maps. The CT scan used a slice thickness of 3.75 mm and a matrix size 512×512. The scan parameters included kVp=120 and variable smart milliAmpere. For CT dose calculation, we used two methods: the DLP (Dose-Length Product) based method and NCICT software. Based on CTDIvol and scan length, DLP uses a simple formula with a conversion factor (K) for tissue sensitivity [27]. NCICT, while undefined in the document, likely employs a more complex algorithm considering patient-specific factors for potentially more accurate dose estimation. Both methods showed consistent results in the study, indicating reliable dose calculations. NCICT offers a more detailed approach by incorporating additional variables affecting radiation dose.

Method 1: Calculating Effective Dose via DLP: Each CT dose report specifies the DLP value for each individual. The system calculates DLP by multiplying the CTDIvol (Computed Tomography Dose Index volume) along the scan length. CTDIvol represents the average absorbed dose in the Z-axis resulting from consecutive axial slices [28]. Conversely, DLP reflects the total radiation received by the scanned body region [29]. To determine the effective dose, the following formula is used (Equation 5):

$$E = DLP \times k \quad (5)$$

Where:

E is the effective dose (in millisieverts, mSv),

DLP is the dose length product (in milligray centimeters, mGy·cm),

k is the conversion factor (here considered 0.015 mSv/mGy·cm for the adult body).

Calculating Effective Dose via NCICT: To evaluate the effective dose using the NCICT software, we consider the following parameters for each patient:

Body size (tabulated value), Adult age group, Gender, mAs (milliampere-seconds), Scanner details: GE manufacture, OPTIMA600 model, body filter, Abdomen protocol with a scan length of 102 cm (covering from slice 4 to 105).

3. Results

3.1. ^{64}Cu-DOTA-Trastuzumab Obtained Image Analysis

The administered activity's mean and Standard Deviation (SD) were 210± 22 MBq (179-227 MBq). All subjects tolerated the administration of 64Cu-DOTA-trastuzumab well, with no reported drug-related adverse events. Furthermore, no clinically significant trends suggestive of a safety signal were observed in laboratory parameters, vital signs, or electrocardiogram readings for the patients included in this study.

Figure 3 depicts whole-body ^{64}Cu-DOTA-trastuzumab PET images gained 1, 12, and 48 hours after injection.

Figure 4 shows the time-activity curves of ^{64}Cu-DOTA-trastuzumab in various tissues of the three patients who participated in the study. The graph likely has the time points (1, 12, and 48 hours after injection) on the x-axis and the Standardized Uptake Value (SUV) on the y-axis. Each curve represents the liver, kidney, lung, heart, and spleen.

Liver, Kidney, and Spleen: These curves show the expected bio-distribution of the radiolabeled antibody in these well-perfused organs. The SUV values are relatively stable, showing that these organs take up and keep the antibody to some extent.

Comparing other radiopharmaceuticals, such as FDG and Ga-PSMA, would involve looking at the patterns of uptake and retention. For instance, FDG is known for its rapid uptake in metabolically active tissues, including many cancers, and, therefore, often yields high-quality images within one hour after injection. In contrast, the study found that ^{64}Cu-DOTA-Trastuzumab does not produce high-quality images within one hour post-injection, suggesting slower kinetics than FDG.

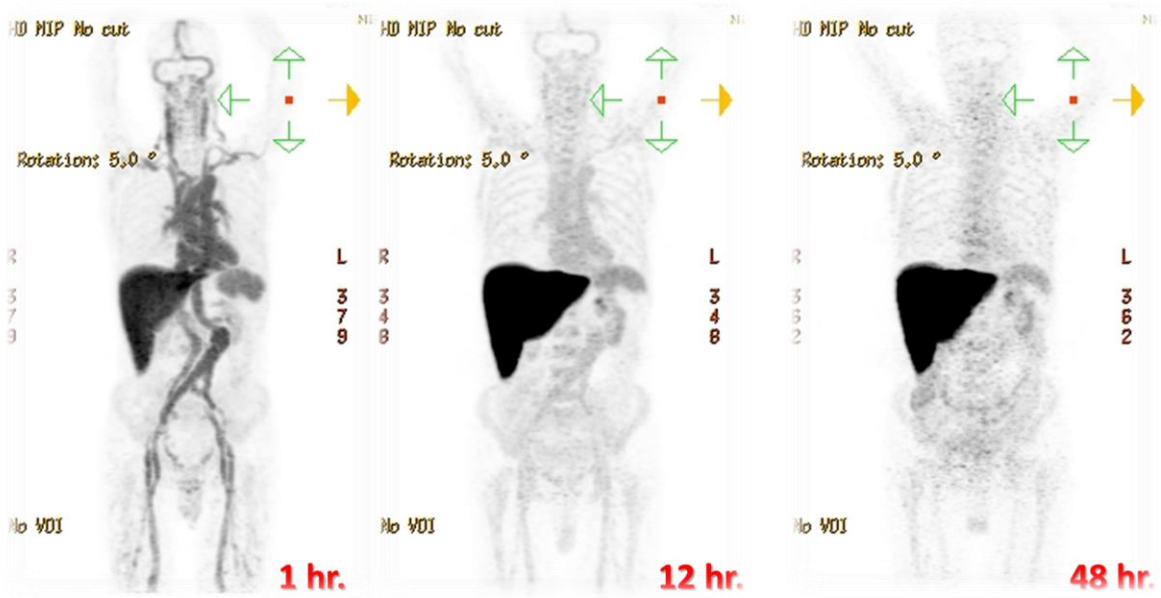

Figure 3. Whole-body 64Cu-DOTA-trastuzumab PET images were acquired at 1, 12, and 48 hours after injection

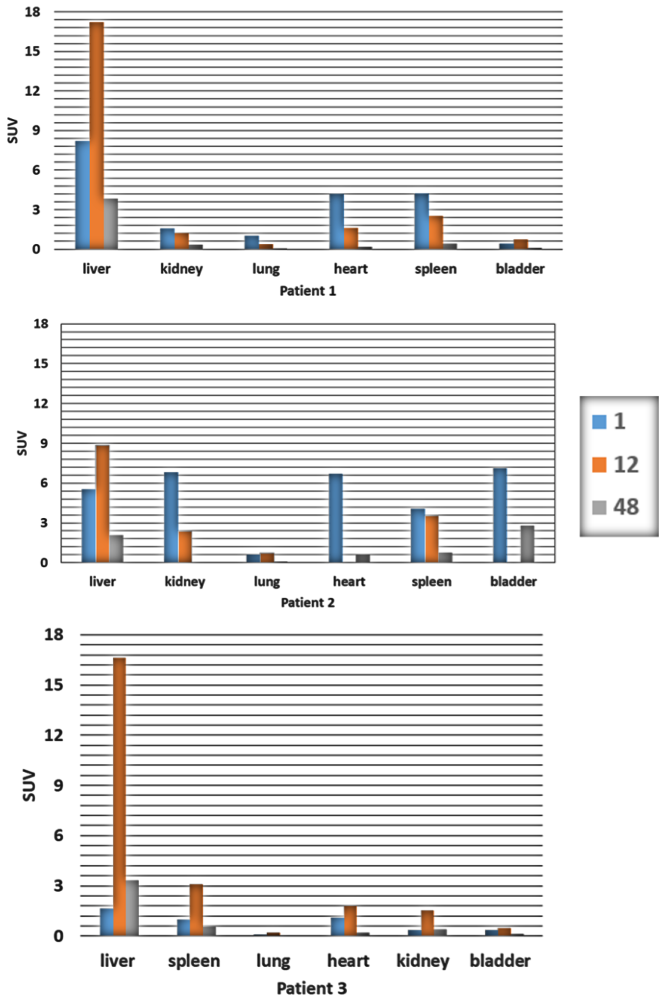

Figure 4. The organ biological distribution and time–activity curves of ^{64}Cu-DOTA-trastuzumab were analyzed in three patients. SUVs in the liver, kidney, lung, heart, spleen, and bladder were calculated based on region-of-interest analysis for each tissue

Therefore, a significant amount of time must elapse post-injection to observe enhanced uptake in organs and tumors. Notably, imaging performed 12 hours or more after injection provides excellent signal-to-noise ratios in organs and may be an optimal time for imaging.

3.2. Bio-Distribution and Absorbed Dose Results

Internal dosimetry was evaluated in all three patients. Cumulative activity per unit of administered activity for kidneys, liver, lungs, and spleen is shown in Table 1, which shows that the liver has higher cumulative activity than other organs. The organ-absorbed effective doses are shown in Table 2. The highest absorbed dose was in the liver, followed by the spleen and other organs, as shown in the table. The average effective dose was estimated to be 7.55E-03±5.66E-04 and 8.85E-03±7.53E-04 mSv/MBq based on ICRP 60 and 103, respectively.

Table 1. Cumulative activity per unit of administered activity

Organs [Ãs/A0]	Patient 1	Patient 2	Patient 3
Kidneys	4.49E-02	8.19E-02	1.93E-02
Liver	2.36E+00	1.57E+00	2.12E+00
Lungs	1.96E-01	5.02E-01	1.07E-01
Spleen	4.44E-02	1.58E-01	3.85E-02

3.3. CT Dose Results

The results of the CT dose calculation for all three patients according to the patient's conditions and CT scanner protocol for those patients are presented in Table 3. As obtained from CT dose calculation, it is clear that the thyroid, salivary glands, and testicles receive high doses in men. In women, because of the high sensitivity of women to radiation, the dose of the organs is higher; in general, the dose obtained by the analytical method based on DLP is equal to 4.3, 7.3, and 5.2 mSv, and from the NCICT method, 4.9, 7.9, and 5.9 mSv for patients 1 to 3 were obtained, respectively.

4. Discussion

The study's main objective was to evaluate the absorbed doses specific to patients who received ^{64}Cu-DOTA-Trastuzumab for PET/CT imaging in cases of gastric cancer. The investigation aimed to enhance understanding of the biokinetic distribution and absorbed dose of ^{64}Cu, essential for its safe and practical application in nuclear medicine.

The production and purification of ^{64}Cu were successfully achieved, and the radiopharmaceutical ^{64}Cu-DOTA-Trastuzumab was prepared with high radiochemical purity, as confirmed by HPLC and ITLC methods [18]. This is crucial for ensuring the imaging results' reliability and the patient's safety. The study's findings on the bio-distribution and dosimetry of ^{64}Cu-DOTA-Trastuzumab in cancer patients provide valuable insights into the pharmacokinetics of this radiopharmaceutical and its potential clinical implications. The administered activity range and the patient's tolerance to the radiopharmaceutical with no reported adverse events suggest that the dosing regimen is safe and well-tolerated.

The PET imaging results at different time points post-injection highlight the importance of considering the pharmacokinetics of the radiopharmaceutical when scheduling PET/CT scans [30]. The observation that imaging at 12 hours or more post-injection yields better signal-to-noise ratios in organs and tumors is significant for optimizing the diagnostic accuracy of PET/CT scans in clinical practice. This finding is particularly relevant given that radiopharmaceuticals do not produce high-quality images within one hour after injection [31]. The bio-distribution data, as depicted in the time-activity curves, show that the liver, kidney, and spleen exhibit expected uptake and retention of the radiolabeled antibody. The relatively stable SUV values in these organs indicate that they are well-perfused and capable of retaining the radiopharmaceutical, consistent with their known biology. The internal dosimetry evaluation reveals that the liver has the highest cumulative activity, followed by the spleen and other organs [32]. This pattern of bio-distribution is expected, given the liver's role in metabolizing and clearing various substances, including antibodies, from the bloodstream [33]. The effective dose estimates for the radiopharmaceutical are within acceptable limits, as indicated by the

Table 2. Estimated Organ-Absorbed Dose and Effective Dose from Whole-Body 64Cu-DOTA-Trastuzumab PET Imaging

Organs [mGy/MBq]	Patient 1	Patient 2	Patient 3	Organs [mGy/MBq]	Patient 1	Patient 2	Patient 3
Bronchi sequestered	6.47E-03	8.07E-03	4.70E-03	Prostate	1.08E-04	8.30E-05	9.37E-05
Bronchioles	1.69E-02	3.47E-02	1.06E-02	Recto-sigmoid colon wall	2.21E-04	1.72E-04	1.91E-04
Colon wall	2.75E-03	2.10E-03	2.40E-03	Red (active) bone marrow	2.25E-03	1.89E-03	1.89E-03
Endosteum (bone surface)	8.52E-04	7.20E-04	7.16E-04	Right colon wall	4.75E-03	3.35E-03	4.19E-03
ET region	2.85E-04	2.75E-04	2.26E-04	Salivary glands	2.74E-04	2.66E-04	2.18E-04
ET1 basal cells	1.94E-04	1.62E-04	1.61E-04	Skin	6.18E-04	5.10E-04	5.25E-04
ET2 basal cells	2.85E-04	2.75E-04	2.26E-04	Small intestine wall	1.96E-03	1.55E-03	1.69E-03
Eye lenses	1.50E-04	1.37E-04	1.23E-04	Spleen	1.79E-02	5.71E-02	1.53E-02
Gallbladder wall	2.50E-02	1.69E-02	2.23E-02	Stomach wall	6.93E-03	5.18E-03	5.94E-03
Heart wall	4.66E-02	4.85E-03	3.25E-02	Testes	2.78E-05	2.12E-05	2.41
Muscle	8.43E-04	7.27E-04	7.10E-04	Thymus	2.55E-03	2.38E-03	1.90
Oesophagus	5.82E-03	4.06E-03	4.66E-03	Thyroid	1.13E-03	1.20E-03	8.60
Oral mucosa	2.74E-04	2.50E-04	2.21E-04	Tongue	2.90E-04	2.66E-04	2.33
Ovaries	0.00E+00	0.00E+00	0.00E+00	Tonsils	1.85E-04	1.76E-04	1.49
Muscle	8.43E-04	7.27E-04	7.10E-04	Ureters	1.75E-03	1.42E-03	1.48
Oesophagus	5.82E-03	4.06E-03	4.66E-03	Urinary bladder wall	2.04E-04	1.55E-04	1.77
Pancreas	9.62E-03	6.81E-03	8.47E-03	Uterus/cervix	0.00E+00	0.00E+00	0.00
Pituitary gland	9.62E-05	9.24E-05	7.55E-05	**Effective dose 60 [mSv/MBq]**	8.15E-03	7.70E-03	6.79
				Effective dose 103 [mSv/MBq]	9.53E-03	9.22E-03	7.80

average practical dose values based on ICRP 60 [34, 35] and 103 [36].

Our research group's study on using ^{64}Cu-DOTA-trastuzumab PET imaging in gastric cancer patients presents findings consistent with and distinct from previous research in the field. Our results indicate that imaging at 12 hours or more post-injection offers superior image quality, which aligns with the consensus that later imaging time points can improve the visualization of the tumor due to increased target-to-background contrast. This finding is in agreement with the study by Tamura *et al.* [37], which identified 48 hours post-injection as the optimal time for assessing tumor uptake in breast cancer patients. The similarity in optimal imaging timing between our gastric cancer study and the breast cancer study by Tamura *et al.* suggests that the pharmacokinetics of ^{64}Cu-DOTA-trastuzumab may be consistent across different types of HER2-positive cancers.

Our observation that the liver exhibited the highest cumulative activity, followed by the spleen and other organs, is not surprising, given their physiological role in the metabolism and clearance of antibodies. This biodistribution pattern is consistent with the findings of Tamura *et al.* [37], who also noted high uptake in the liver and other well-perfused organs. However, the specific organ distribution and kinetics may vary depending on the cancer type and individual patient characteristics, which warrants further investigation.

The effective dose estimates for ^{64}Cu-DOTA-trastuzumab in our study were within acceptable limits, as defined by the International Commission on Radiological Protection (ICRP). This finding is

Table 3. Organ doses and effective dose obtained from CT in PET-CT examination

	Patient 1	Patient 2	Patient 3
AGE	61	65	69
Patient weight	55	62	58
Patient height	1.6	1.55	1.79
mA	75	121	92
CTDI(v)(mGy)	2.81	4.53	3.43
DLP(mGy-cm)	326.01	524.9	397.35
Brain	4	7.19	4.88
Pituitary gland	3.64	6.85	4.45
Lens	4.98	8.14	6.08
Eyeballs	4.83	8.18	5.9
Salivary glands	5.1	8.44	6.22
Oral cavity	5.06	8.15	6.18
Spinal cord	4.53	7.71	5.53
Thyroid	6.12	11.23	7.47
Esophagus	4.24	7.44	5.17
Trachea	4.54	7.74	5.54
Thymus	4.49	7.93	5.49
Lungs	4.51	7.85	5.51
Breast	4.02	6.87	4.9
Heart wall	4.71	7.99	5.75
Stomach wall	4.69	8.48	5.73
Liver	4.76	8.4	5.81
Gall bladder	4.41	7.82	5.38
Adrenals	4.24	7.44	5.17
Spleen	4.78	8.44	5.83
Pancreas	4.2	7.83	5.13
Kidney	4.93	9.27	6.02
Small intestine	4.27	7.75	5.21
Colon	4.85	8.54	5.92
Rectosigmoid	3.87	5.98	4.72
Urinary bladder	4.14	6.71	5.05
Prostate	4.46	0	5.44
Uterus	0	5.45	0
Testes	5.33	0	6.51
Ovaries	0	6.25	0
Skin	3.15	5.63	3.84
Muscle	0.15	0.47	0.18
Active marrow	3.43	6.05	4.19
Shallow marrow	3.33	6.55	4.06
Effective dose(mSv)	**4.32**	**7.34**	**5.28**
Effective dose(mSv) formul	**4.89**	**7.87**	**5.96**

reassuring and supports the radiopharmaceutical's safety profile. Tamura *et al.* [37] also reported that the radiation exposure from ^{64}Cu-DOTA-trastuzumab PET was comparable to that of conventional ^{18}F-FDG PET, further validating the safety of this imaging modality.

Interestingly, our CT dose calculations revealed that sensitive organs received higher doses, which could be attributed to the higher energy of the CT scan compared to the PET component. This finding underscores the importance of considering the cumulative radiation dose from both PET and CT when performing PET/CT scans, especially in the context of repeated imaging for cancer management.

The CT dose results demonstrate that sensitive organs such as the thyroid, salivary glands, and testicles receive higher doses. The consistency in the dose estimates obtained from the analytical method based on DLP and the NCICT method provides confidence in the accuracy of the dose calculations.

Finally, while ^{64}Cu-DOTA-Trastuzumab holds promise, its use is still under investigation. Clinical trials are necessary to fully understand its efficacy, safety profile, and optimal dosing. Additionally,

producing and handling radioactive materials require specialized facilities and expertise, which may limit its availability.

5. Conclusion

In conclusion, the study's findings underscore a prizing understanding of the bio-kinetic distribution and absorbed dose of ^{64}Cu-DOTA-Trastuzumab for its safe and effective use in cancer imaging. The optimal timing for PET/CT imaging and the dosimetry data provided by this study can guide clinicians in making informed decisions about using this radiopharmaceutical in patient care. Further research is needed to explore the therapeutic potential of ^{64}Cu-DOTA-Trastuzumab and to establish guidelines for its use in clinical practice.

Acknowledgments

This work was supported under [Grant Number: 57673], Tehran University of Medical Sciences, Tehran, Iran. This research project has been conducted in accordance with the ethical code IR.TUMS.MEDICINE.REC.1401.529. We acknowledge that we used an AI-powered paraphrasing tool to rephrase some parts of our original text to enhance the grammatical accuracy and overall writing quality of this article.

References

1- Y. Zhou *et al.*, "(64)Cu-based Radiopharmaceuticals in Molecular Imaging." (in eng), *Technol Cancer Res Treat,* Vol. 18p. 1533033819830758, Jan 1 (2019).

2- M. Shokeen and C. J. Anderson, "Molecular imaging of cancer with copper-64 radiopharmaceuticals and positron emission tomography (PET)." (in eng), *Acc Chem Res,* Vol. 42 (No. 7), pp. 832-41, Jul 21 (2009).

3- J. P. Holland, R. Ferdani, C. J. Anderson, and J. S. Lewis, "Copper-64 Radiopharmaceuticals for Oncologic Imaging." (in eng), *PET Clin,* Vol. 4 (No. 1), pp. 49-67, Jan (2009).

4- B. Grubmüller *et al.*, "(64)Cu-PSMA-617 PET/CT Imaging of Prostate Adenocarcinoma: First In-Human Studies." (in eng), *Cancer Biother Radiopharm,* Vol. 31 (No. 8), pp. 277-86, Oct (2016).

5- C. J. Anderson and R. Ferdani, "Copper-64 radiopharmaceuticals for PET imaging of cancer: advances in preclinical and clinical research." (in eng), *Cancer Biother Radiopharm,* Vol. 24 (No. 4), pp. 379-93, Aug (2009).

6- Lei Jiang *et al.*, "Pilot Study of 64Cu(I) for PET Imaging of Melanoma." *Scientific Reports,* Vol. 7 (No. 1), p. 2574, 2017/05/31 (2017).

7- B. Gutfilen, S. A. Souza, and G. Valentini, "Copper-64: a real theranostic agent." (in eng), *Drug Des Devel Ther,* Vol. 12pp. 3235-45, (2018).

8- C. Bailly *et al.*, "Comparison of Immuno-PET of CD138 and PET imaging with (64)CuCl(2) and (18)F-FDG in a preclinical syngeneic model of multiple myeloma." (in eng), *Oncotarget,* Vol. 9 (No. 10), pp. 9061-72, Feb 6 (2018).

9- M. N. Amiot *et al.*, "Standardization of 64Cu using an improved decay scheme." *Nuclear Instruments and Methods in Physics Research Section A: Accelerators, Spectrometers, Detectors and Associated Equipment,* Vol. 684pp. 97-104, 2012/08/21/ (2012).

10- A. Monsef, P. Sheikhzadeh, J. R. Steiner, F. Sadeghi, M. Yazdani, and P. Ghafarian, "Optimizing scan time and bayesian penalized likelihood reconstruction algorithm in copper-64 PET/CT imaging: a phantom study." (in eng), *Biomed Phys Eng Express,* Vol. 10 (No. 4), May 14 (2024).

11- "In This Issue." *Molecular Therapy,* Vol. 25 (No. 12), (2017).

12- Vahidfar Nasim *et al.*, "Recent Advances of Copper-64 Based Radiopharmaceuticals in Nuclear Medicine." in *Advances in Dosimetry and New Trends in Radiopharmaceuticals*, Osibote Ololorin Adelaja and Eppard Elisabeth, Eds. Rijeka: *IntechOpen*, (2024), p. Ch. 5.

13- S. Heidari, M. Sadeghi, M. Akhlaghi, D. Beiki, and S. I. Yazdi, "Internal dosimetry of (64)Cu-DOX-loaded microcapsules by Monte Carlo method." (in eng), *Appl Radiat Isot,* Vol. 196p. 110788, Jun (2023).

14- Tengzhi Liu, Morten Karlsen, Anna Karlberg, and Kathrine Redalen, "Hypoxia imaging and theranostic potential of [64Cu][Cu(ATSM)] and ionic Cu(II) salts: a review of current evidence and discussion of the retention mechanisms." *EJNMMI Research,* Vol. 10p. 33, 04/09 (2020).

15- Francesco Fiz *et al.*, "Diagnostic and Dosimetry Features of [64Cu]CuCl2 in High-Grade Paediatric Infiltrative Gliomas." *Molecular Imaging and Biology,* Vol. 2508/30 (2022).

16- M. A. Avila-Rodriguez *et al.*, "Biodistribution and radiation dosimetry of [(64)Cu]copper dichloride: first-in-human study in healthy volunteers." (in eng), *EJNMMI Res,* Vol. 7 (No. 1), p. 98, Dec 12 (2017).

17- J. E. Mortimer *et al.*, "Use of (64)Cu-DOTA-Trastuzumab PET to Predict Response and Outcome of Patients Receiving Trastuzumab Emtansine for Metastatic

Breast Cancer: A Pilot Study." (in eng), *J Nucl Med,* Vol. 63 (No. 8), pp. 1145-48, Aug (2022).

18- Copper-64 Radiopharmaceuticals: Production, Quality Control and Clinical Applications. Vienna: *INTERNATIONAL ATOMIC ENERGY AGENCY*, (2022).

19- C Nioche, F Orlhac, S Boughdad, S Reuzé, J Goya-Outi, C Robert, C Pellot-Barakat, M Soussan, F Frouin, and I Buvat. "LIFEx: a freeware for radiomic feature calculation in multimodality imaging to accelerate advances in the characterization of tumor heterogeneity." *Cancer Research*; 78(16):4786-4789, (2018).

20- Al-Fatlawi, Murtadha, Farideh Pak, Saeed Farzanefar, Yalda Salehi, Abbas Monsef, and Peyman Sheikhzadeh. "Optimization of the Acquisition Time and Injected Dose of 18F-Fluorodeoxyglucose Based on Patient Specifications for High-Sensitive Positron Emission Tomography/Computed Tomography Scanner." *World Journal of Nuclear Medicine 22*, no. 03: 196-202, (2023)."

21- Sara Neira *et al.*, "Quantification of internal dosimetry in PET patients: individualized Monte Carlo vs generic phantom-based calculations." *Medical Physics,* Vol. 47 (No. 9), pp. 4574-88, (2020).

22- M. Karimipourfard, S. Sina, and M. S. Alavi, "Toward three-dimensional patient-specific internal dosimetry using GATE Monte Carlo technique." *Radiation Physics and Chemistry,* Vol. 195p. 110046, 2022/06/01/ (2022).

23- Cassandra Métivier *et al.*, "Preclinical Evaluation of a 64Cu-Based Theranostic Approach in a Murine Model of Multiple Myeloma." *Pharmaceutics*. Vol. 15 (No. 7). DOI: 10.3390/pharmaceutics15071817

24- S. Soongsathitanon, P. Masa-Ah, and Malulee Tuntawiroon, "A new Standard Uptake Values (SUV) calculation based on pixel intensity values." Vol. 6pp. 26-33, 01/01 (2012).

25- M. Andersson, L. Johansson, K. Eckerman, and S. Mattsson, "IDAC-Dose 2.1, an internal dosimetry program for diagnostic nuclear medicine based on the ICRP adult reference voxel phantoms." (in eng), *EJNMMI Res,* Vol. 7 (No. 1), p. 88, Nov 3 (2017).

26- Matthew Large, Alessandra Malaroda, Marco Petasecca, Anatoly Rosenfeld, and S. Guatelli, Modelling ICRP110 Adult Reference Voxel Phantoms for dosimetric applications: Development of a new Geant4 Advanced Example. (2020).

27- Samira Kamrani, Nima Kasraie, Fatemeh Jahangiri, Davood Khezrloo, and Peyman Sheikhzadeh, "Organ doses, effective dose, and cancer risk estimation from head and neck CT scans." *Radiation Physics and Chemistry,* Vol. 212p. 111163, 07/01 (2023).

28- C. Anam, F. Haryanto, R. Widita, I. Arif, G. Dougherty, and D. McLean, "Volume computed tomography dose index (CTDIvol) and size-specific dose estimate (SSDE) for tube current modulation (TCM) in CT scanning." *Int-J-Radiat-Res,* Vol. 16 (No. 3), pp. 289-97, (2018).

29- I. Lange, B. Alikhani, F. Wacker, and H. J. Raatschen, "Intraindividual variation of dose parameters in oncologic CT imaging." (in eng), *PLoS One,* Vol. 16 (No. 4), p. e0250490, (2021).

30- Rubel Chakravarty, Hao Hong, and Weibo Cai, "Positron Emission Tomography Image-Guided Drug Delivery: Current Status and Future Perspectives." *Molecular Pharmaceutics,* Vol. 11 (No. 11), pp. 3777-97, 2014/11/03 (2014).

31- Sally Pimlott and Andrew Sutherland, "Molecular tracers for the PET and SPECT imaging of disease." *Chemical Society reviews,* Vol. 40pp. 149-62, 04/19 (2011).

32- Samira Heidari, Mahdi Sadeghi, Mehdi Akhlaghi, Davood Beiki, and Saeideh Yazdi, "Internal dosimetry of 64Cu-DOX-loaded microcapsules by Monte Carlo method." *Applied Radiation and Isotopes,* Vol. 196p. 110788, 03/01 (2023).

33- A. W. Wong *et al.*, "A comparison of image contrast with (64)Cu-labeled long circulating liposomes and (18)F-FDG in a murine model of mammary carcinoma." (in eng), *Am J Nucl Med Mol Imaging,* Vol. 3 (No. 1), pp. 32-43, (2013).

34- P. S. Iyer, "Current radiation protection standards: ICRP-60." *Indian Journal of Radiology and Imaging,* Vol. 5 (No. 2), pp. 81-83, (1995).

35- Karimipourfard, M., S. Sina, and M. S. Alavi. "Toward three-dimensional patient-specific internal dosimetry using GATE Monte Carlo technique." *Radiation Physics and Chemistry* 195, 110046, (2022).

36- Jean-Claude Nenot, Jean Brenot, Dominique Laurier, Alain Rannou, and Dominique Thierry, "ICRP Publication 103 The 2007 Recommendations of the International Commission on Radiological Protection." France, 978-2-7430-1120-8, (2009), [Online]. Available: http://inis.iaea.org/search/search.aspx?orig_q=RN:49042116.

37- K. Tamura *et al.*, "64Cu-DOTA-trastuzumab PET imaging in patients with HER2-positive breast cancer." (in eng), *J Nucl Med,* Vol. 54 (No. 11), pp. 1869-75, Nov (2013).